Microneedle-based precision payload delivery in plants

Mingzhuo Li[1], Aditi Dey Poonam[1], Deepjyoti Singh[2], Jin Xu[1], Hongwei Jing[4], Ziwei Zuo[5], Yipeng Huang[6], Nana Liu[6], Yajun Liu[5], Liping Gao[5], Tao Xia[6], Anna E. Whitfield[2,3], and Qingshan Wei[1,3] *

1. Department of Chemical and Biomolecular Engineering, North Carolina State University, Raleigh, NC 27695
2. Department of Entomology and Plant Pathology, North Carolina State University, Raleigh, NC, 27606
3. Emerging Plant Disease and Global Food Security cluster, North Carolina State University, Raleigh, NC 27695
4. Department of Horticultural Science, North Carolina State University, Raleigh, NC, 27606
5. Department of Biological Sciences, School of Life Science, Anhui Agricultural University, No. 130, West Changjiang Road, Hefei 230036, Anhui, China
6. State Key Laboratory of Tea Plant Biology and Utilization, Anhui Agricultural University, No. 130, West Changjiang Road, Hefei 230036, Anhui, China

* Corresponding email: qwei3@ncsu.edu

Running title: **Precision molecular delivery to live plants with microneedles**

Abstract:

Traditional crop delivery methods, such as foliar spray and soil application, face significant limitations, including nutrient loss, environmental impacts, and low delivery efficiency. Recent advances in nanomaterials have offered novel molecular delivery platforms, but challenges such as synthesis complexity, long-term stability, and compliance with rigorous biosafety regulations persist. To provide a simpler, lower-cost, and safer alternative, we developed a polyvinyl alcohol (PVA)-based microneedle (MN) delivery system that can be precisely applied to various plant tissues (e.g., stem, lateral branch, or petiole), which demonstrates high delivery efficiency compared to the conventional methods (3.5x higher tissue accumulation) while reducing application dose (>90% less). This MN system facilitates the delivery of diverse small molecules, ranging from fluorescent dyes, growth promoters, to antiviral hormones, into plant tissues, on the other hand showing limited wounding stress to the plant. By applying fluorescent dye-loaded MNs onto tomato stems, we demonstrated effective molecular diffusion through vascular tissues. Additionally, MNs loaded with gibberellic acid (GA3) enhanced stem and branch growth in tomatoes and restored the lateral flowering phenotype in *Arabidopsis ft-10* mutants, with significant upregulation of GA receptor gene expression. Lastly, salicylic acid (SA) injections with MNs induced resistance to tomato spotted wilt virus (TSWV) in *Nicotiana benthamiana*, comparable to conventional spray and infiltration-based approaches. This easily fabricated and cost-effective MN system offers a promising tool for precision agriculture, enhancing plant health and productivity while significantly reducing the use of agrochemicals.

Keywords: plant delivery, microneedle, phytohormone, pathogen resistance, precision agriculture

Introduction:

Currently, two of the most widely used methods for active delivery in agriculture are foliar spray and soil application (Niu et al., 2021; Nkebiwe et al., 2016). These two methods are popular due to their simplicity, speed, and ease of scaling up. However, with the ongoing development of the agricultural industry, significant limitations of these traditional delivery methods have become apparent (Sinha et al., 2022; Zheng et al., 2020). As larger areas of cropland and a wider variety of crops are integrated into the agricultural industry to meet the increasing food demands driven by rapid population growth, these methods of conventional compound application face new challenges (Davis et al., 2016; Fukase and Martin, 2020).

A major limitation of the foliar application method lies in its relatively low deposition efficiency and high loss of active compounds before reaching the target plant tissues. Using pesticides as an example, about 30–50% of them are dispersed into the air during the spraying process (Boonupara et al., 2023). Under unfavorable surface conditions, the deposition efficiency of foliar sprays can drop to as low as ~20%, meaning that the majority of the applied chemicals fail to adhere to the leaf surface (Zhang et al., 2023).

While soil application saves more chemicals or nutrients, it still results in significant losses due to factors such as leaching, runoff, and volatilization. Field studies have reported that nitrogen (N) losses can range from approximately 3% to >15% of the applied amount, depending on crop type, soil properties, and management practices. For example, in a paddy field in southern China, about 3.32% of applied N was lost via surface runoff, with an additional 4.8% lost through subsurface leaching (Zeng et al., 2021). Similarly, in the Yellow River irrigation area in China, the use of conventional nitrogen fertilizers led to total N leaching loss of up to 17.7% (He et al., 2025).

Foliar application and soil-based treatment also pose significant environmental concerns when applied in high volume or under sub-optimal timing. While these methods offer convenience for crop uptake, runoff or leaching from rainfall or irrigation events can result in active compounds entering adjacent water bodies or deeper soils. For example, a new meta-analysis shows that nitrogen fertilizers (both synthetic and organic) contribute to significant nitrate leaching into groundwater, especially in coarse-textured soils and certain crop systems (Hina, 2024). Large amounts of chemicals applied to the soil can result in water contamination, soil acidification, salinization, and structural change, and eventually negative impacts to biodiversity in the soil

(Alkharabsheh et al., 2021; Brichi et al., 2023; Young et al., 2021). A recent study in southwestern Germany detected large amounts of pesticides (including insecticides) in surface waters within protected areas (Schemmer et al., 2024).

In addition to generating waste and imposing environmental pressures, traditional fertilizer methods face further limitations due to the crop's internal structure: the crop leaf cuticle, which acts as a barrier, slows down nutrient and chemical absorption (Barłóg et al., 2022; Krishnasree et al., 2021; Vasundhara and Chhabra, 2021). As such, the foliar spray approach often provides only short-term relief from nutrient deficiencies and requires frequent reapplications. Similarly, soil fertilization exhibits low efficiency, as plant uptake is delayed while nutrients move through the soil matrix into the root tissue, and it can also lead to uneven nutrient distribution (Barłóg *et al.*, 2022; Dimkpa et al., 2020).

In recent years, several approaches have been developed to address these limitations in traditional crop delivery systems to make molecular delivery in plants more effective. One example of emerging technology is the use of nanomaterials as a plant delivery system (Beig et al., 2022; Jakhar et al., 2022; Liu et al., 2021; Salama et al., 2021). Nanomaterials show characteristics that protect labile compounds from fast degradation, increase the adhesion of payloads to plants, control the release of payloads, and enhance the permeability of payloads through the cuticle or internalization into plant tissues or cells (Cunningham et al., 2018; Nair et al., 2010). For example, nanocarriers (e.g., carbon nanotubes, quantum dots, and metal/metal oxide NPs) are designed to deliver DNA molecules to perform plant genome engineering, such as gene transformation, siRNA silencing, and gene editing (Cunningham *et al.*, 2018; Nair *et al.*, 2010; Wang et al., 2021; Zhang et al., 2021; Zhang et al., 2022; Zhang et al., 2020). However, most of these nanoscale genetic molecular delivery methods are limited by the complex nanomaterial design. In addition, the toxicity of nanoparticles to plants and animals remains a significant concern (Cunningham *et al.*, 2018). Furthermore, these methods are commonly applied by spraying, which suffers from the same low uptake efficiency (~0.1% for root application and <30% via leaf) (Tudi et al., 2021). Alternative delivery methods, such as foliar infiltration, are labor-intensive and leaf-restricted, limiting their use in the field and for broad plant species.

The microneedle (MN) is a new technique that has been applied to precision agriculture recently (Jung and Jin, 2021; Nagarkar et al., 2020). MN refers to microscopic needles, typically

113 ranging from 150 to 1500 μm in length, 50 to 250 μm in base width, and 1 to 25 μm in tip diameter.
114 MNs can be applied to plant tissues for the delivery of essential compounds such as nutrients,
115 metabolites, and agrochemicals, thereby improving plant health and productivity (Ece et al., 2023;
116 Faraji Rad, 2023). A previous example of MNs for plant delivery is biocompatible silk MNs
117 developed for precision delivery of pesticides and other essential compounds into plants (Cao et
118 al., 2023; Cao et al., 2020; Han et al., 2025). Even though this silk-based MN provides a new tool
119 to deliver physiologically functional compounds into crops, the source of materials and fabrication
120 process limit its wide application in large-scale agricultural activities. In our previous study, we
121 developed a different MN system using water-soluble and biocompatible polyvinyl alcohol (PVA)
122 as the base material (Paul et al., 2021; Paul et al., 2020; 2022). The PVA-based MN effectively
123 isolated genetic molecules (e.g., DNA and RNA) from plant tissues, demonstrating its potential
124 for use in early and in-field crop disease diagnostics (Paul *et al.*, 2020; 2022). More recently, we
125 also applied PVA MNs to crop seeds (e.g., soybeans), and demonstrated their capability for rapid
126 seed DNA extraction for genotyping and whole genome sequencing, a much-simplified trait
127 analysis technology that can greatly speed up the breeding process (Li et al., 2025)

128 In this study, we explored the capability of cost-effective and easy-to-scale-up PVA- MN
129 to deliver small molecules into plant systems. We first tested the wounding stress induced by the
130 PVA-MN treatment on plants and characterized the diffusion behavior of fluorescent dyes from
131 the MN tips into tomato stem vascular tissues. Then, we demonstrated the MN-assisted delivery
132 of plant hormone gibberellic acid (GA3) to promote plant growth and restore lateral flowering in
133 Arabidopsis *ft-10* mutants. Finally, we tested the delivery of salicylic acid (SA) to the model plant
134 *Nicotiana Benthamiana* to inhibit the transportation of tomato spotted wilt virus (TSWV).
135 Together, these results demonstrated PVA- MN's effectiveness in delivering small molecules,
136 particularly plant hormones, to plants. This PVA- MN system holds great promise for future
137 applications in precision agriculture.

138

139 **Results:**

140 Tomato was chosen as the model system due to its well-defined vascular structure and long petioles.
141 Previous studies have shown that the segment between the vasculature and the epidermis ranges
142 from 840–1040 μm for xylem and 707–925 μm for phloem in tomato plants, with xylem and

143 phloem diameters in the tens and hundreds of micrometers, respectively (Cao *et al.*, 2020). Based
144 on these parameters, we designed and fabricated a 1000-μm-long PVA-MN as a microinjector to
145 study payload delivery in planta (Figure 1A).

146

147 **Effect of MN-induced mechanical stress on plant growth**

148 PVA is a synthetic polymer with several distinct characteristics, such as water solubility,
149 biodegradability, non-toxicity, and tunable mechanical properties, making it a promising candidate
150 for applications in plant delivery. To test whether PVA MN could be used for chemical delivery
151 in plant tissue, we first examined its mechanical damage to plant health. Due to the strong
152 hygroscopic nature of PVA, we observed that leaf tissues punctured by the PVA MN dehydrated
153 rapidly if the MN was not removed immediately after penetration (e.g., contact time >20 s),
154 causing surrounding tissues to wilt within an hour post-puncture (Figure S1). In contrast, when the
155 microneedle was applied to the stem, although localized dehydration occurred at the puncture site,
156 the vascular bundles remained largely unaffected and continued to function properly (Figure S1).
157 These results indicate that the microneedle contact time for leaf delivery needs to be controlled,
158 whereas the stem is a more robust delivery site for PVA MN.

159 The morphology changes of MN tips before and after stem penetration were characterized
160 by scanning electron microscopy (SEM) (Figure S2A,B). We found that after 30 seconds inside
161 the stem, the MN tips were softened, and some needle tips were partially dissolved by the cellular
162 fluids within the stem. The PVA-MN weight loss was also monitored. Before MN punching on
163 the tomato stem, the average weight of a small PVA-MN patch (9 x 6 array) is around 2.5 mg
164 (Figure S2C). After MN injection, the average weight of used MN is about 7, 10, or 13% lower
165 than that of the new MN patches with contact time of 1, 2, and 15 min, respectively, indicating
166 PVA material dissolving over time during the MN treatment process (Figure S2C). Additionally,
167 we tested the mechanical properties of PVA MN under compression on the stem. The results
168 showed that the average needle tip break force for tomato stem penetration is about 0.2N (Figure
169 S2D). These observations indicate that PVA MN exhibits an excellent combination of rapid water
170 solubility and mechanical strength for plant delivery.

171 Next, we investigated whether the PVA MN punch at the stem would have a negative
172 impact on plant health and growth over time. We examined the damage caused by MN insertion
173 on tomato stems under a microscope (Figure S3). On the punctured surface, the tomato stems
174 appeared slightly hardened, but no visible oxidation or darkening was observed at the puncture
175 sites. This phenomenon could be attributed to PVA's water-absorbing property, which causes local
176 cell dehydration and the formation of a protective layer. The microscopic images of the tomato
177 stem cross-section showed that the pith region at the center of the stem developed a few void zones
178 at 2 mins after MN punch, indicating acute cell damage (Figure S3B, middle column). However,
179 over time, the pith cells repaired themselves and filled these gaps within 48 hours after MN
180 puncturing (Figure S3B, right column). Meanwhile, the vascular bundle cells at the puncture site
181 formed a protective layer upon cell death, which helped prevent further internal damage. In
182 addition, no excessive tissue oxidation or darkening was observed around the puncture site
183 externally (Figure S3, top row).

184 The tomato *SIBOH1*(Respiratory burst oxidase homolog) gene is a commonly used
185 indicator of the abiotic stresses. We analysed the *SIBOH1* gene expression in the stem after the
186 PVA MN punch. The results showed that the transcription level of *SIBOH1* was induced by 2-6
187 fold immediately after MN treatment (30 mins) (Figure S4A). However, the *SIBOH1* expression
188 decreased to a normal level after 48 h of MN punch (Figure S4A). At the same time, we also
189 tracked the *TomLOXD* gene, which is a classical lipoxygenase gene induced by mechanical
190 damage. Gene expression analysis showed that the relative expression level of *TomLOXD* was also
191 induced 3-4 fold after 30 min of MN wounding; after 48 h, the relative expression of *TomLOXD*
192 was down regulated to the normal range (Figure S4B). These molecular results match the previous
193 microscopic observations (Figure S3), suggesting that the MN-treated plant stem showed a certain
194 level of acute mechanical damage, which was eventually self-recovered.

195 Meanwhile, we compared the growth of wild-type (WT) tomato plants (without MN punch)
196 with those that had been subjected to three rounds of PVA-MN puncturing. Phenotypically, there
197 are no significant differences in growth height between WT and MN-treated plants (Figure S5A).
198 Quantitative measurements of plant height were taken at 1, 6, and 15 days after puncturing and
199 revealed no noticeable differences compared with WT plants (Figure S5B). Together, these

200 findings (Figure S3-5) suggest that PVA MN puncturing on tomato plant stems, even with repeated
201 treatments, does not exert a significant inhibitory effect on normal plant growth.

202

203 **Delivery of fluorescent molecules in plant tissue**

204 Fluorescent or colorimetric dyes were chosen as the first model small molecules for MN-assisted
205 plant delivery. Because of the water-dissolving characteristic of the PVA material, we speculated
206 that the small molecules are more likely to be transported by xylem. Safranin is a common plant
207 histological staining dye for xylem ducts. We loaded safranin into the PVA- MN at a concentration
208 of 1%. After stem injection, we observed a faint reddish color accumulation around the vessel cells
209 after MN injection, suggesting that the MN-delivered dyes were mainly transported through the
210 xylem system after MN punching (Figure 1B).

211 We also incorporated fluorescent dyes, such as rhodamine 6G (maximum absorption at 526
212 nm) and 5(6)-carboxyfluorescein diacetate (CFDA, maximum absorption at 492 nm), into the
213 PVA-MN. We observed the diffusion of CFDA into surrounding tissues within 5 minutes of PVA-
214 MN injection (Figure 1C). To analyze molecular transport in the xylem, we performed tangential
215 sectioning of the stem and monitored the dye diffusion at 1-, 5-, and 10-min post-injection by
216 fluorescence imaging. The results showed a significantly more widespread distribution at 5 min
217 post-injection than at 1 min (Figure 1C). Quantification of relative fluorescence intensity showed
218 a 32% and 77% increase of dye diffusion area in stems at 5- and 10-min post-injection, respectively
219 (Figure S6). Additionally, the chemical dyes were observed to travel along the xylem flow in the
220 tomato stem (Figure S7). These findings strongly suggest that the PVA-MN tip effectively reaches
221 the vasculature and that chemical compounds embedded in the PVA-MN can diffuse and be
222 transported along the vascular, especially the vessel cell delivery system in tomato plants.

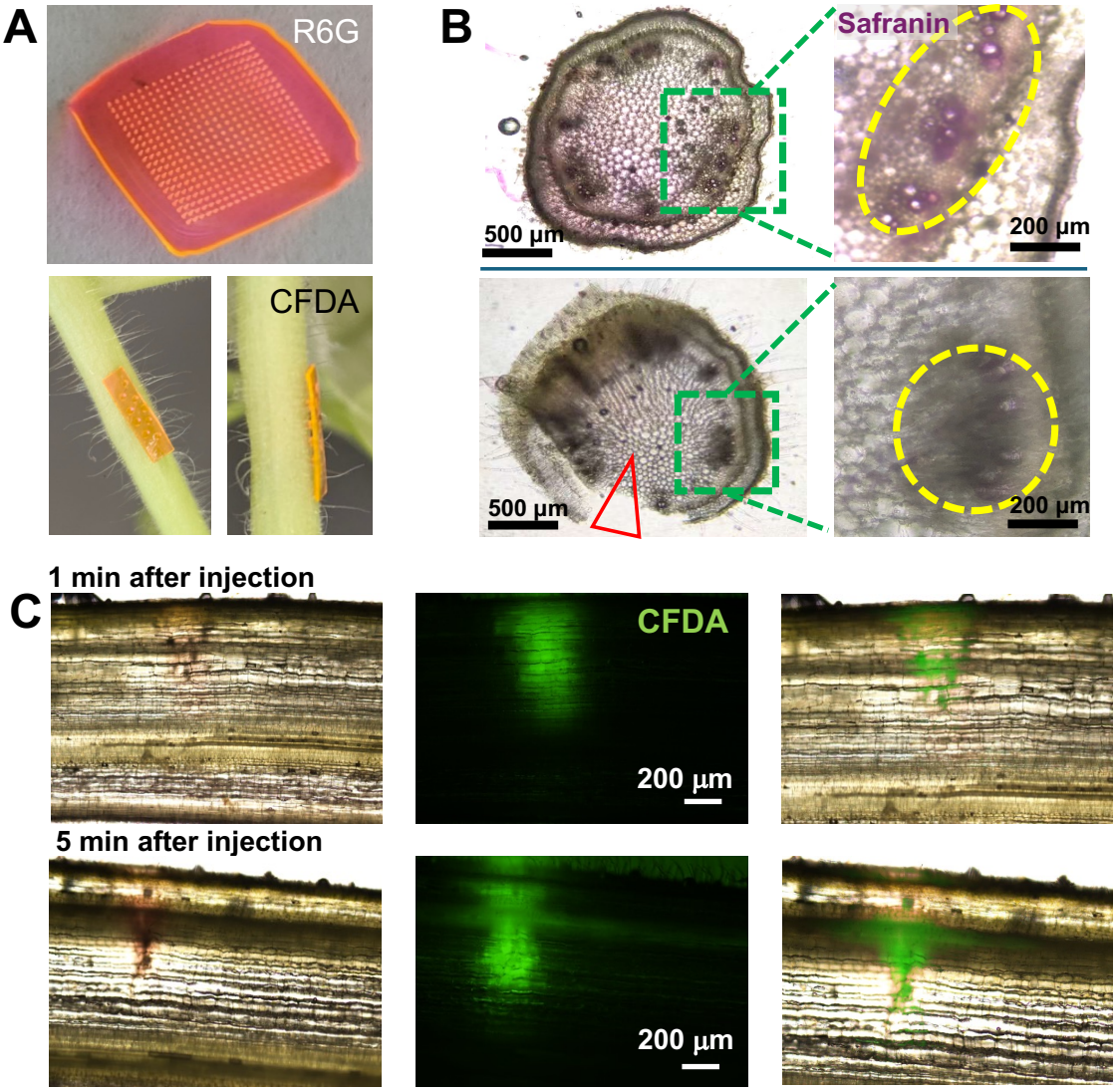

Figure 1: PVA-MN delivery of fluorescent dyes into tomato plant vasculature system. A) Photographs of rhodamine 6G-loaded PVA MN (top) and a PVA patch loaded with 5(6)-carboxyfluorescein diacetate (CFDA), inserted into the tomato stem (bottom). B) Cross-section microscopy images of tomato stems. Top: tomato stem without MN treatment but stained with safranin directly. The reddish cells in the zoomed-in image indicate the vascular sieve cells. Bottom: tomato stem with MN-safranin treatment (12 h). The red arrow indicates the MN penetration position; the zoomed-in image shows the accumulation of safranin dyes in the sieve cells, similar to direct staining. C) Vertical-section microscopy images (from left to right: brightfield, fluorescence, and overlap) showing CFDA delivered and transported along tomato xylem, after 1 min and 5 min of PVA MN injection.

234 **Delivery of growth regulator GA3 to promote tomato plant growth**

235 To demonstrate the utility of PVA MN to deliver plant growth regulators (PGRs) in crops, we
236 investigated the delivery of gibberellic acid (GA3) to tomato plants. GA3 is a plant hormone that
237 plays a crucial role in regulating various growth and developmental processes in plants, such as
238 seed germination, stem elongation, flowering, and fruit development (Gupta and Chakrabarty,
239 2013). In the current study, the tomato stem was selected as the injection site.

240 Twenty-five-day-old tomato plants (n=12) were injected with the PVA-MN on the stem
241 tissue (Figure 2A, Figure S8). Following the initial MN injection, secondary and tertiary injections
242 were performed 3 and 6 days later, respectively. Plants treated with PVA MN without GA3
243 (negative control, or "Control-MN"), plants with direct GA3 injection at the stem by a syringe
244 ("GA3-Injection"), and plants sprayed with GA3 on their leaves (positive control, or "GA3-Spary")
245 were included in the experiment (Figure 2A). In addition, healthy plants without any microneedle
246 or GA3 treatment were used as the wild type ("WT", Figure 2A). The PVA-MN patch contains
247 500 μM GA3, which is higher than the loading concentration of GA3 in the spray method (100
248 μM). At the same time, for direct stem injection, we used 100 μL of GA3 solution with a
249 concentration of 100 μM. However, due to the much smaller delivery volume of the PVA- MN
250 method (only an array of ~ 4 x 10 needles penetrated stems) compared to 5-10 mL of solutions
251 applied in the spray method, three treatments of PVA-MN deliver an estimated total amount of
252 0.05-0.075 μmol of GA3, which is only about 10% of the spray method, and 50% of the stem-
253 based direct injection method (Table1).

254 **Table 1. Comparison of plant hormone consumption in different delivery methods**

Plants	**Cargo**	**Delivery Methods**		
		GA3-MN	GA3-Spary	GA3-Stem Injection
Tomato	GA3	0.05~0.075 μmol	0.5~1 μmol	1~1.5 μmol
Arabidopsis	GA3	0.025~0.03 μmol	0.2~0.4 μmol	
		SA-MN	SA-Spray	SA-Leaf Infiltration
Nicotiana benthamiana	SA	1.2~1.6 μmol	200~250 μmol	50 μmol

255

256

After six days, we observed that tomato plants treated with GA3, including GA3-MN, GA3-Spary, and GA3-Injection, exhibited a faster growth rate compared to control plants (both WT and Control-MN, Figure 2B, C, E). The stem lengths (labeled in red, Figure 2B, C) were quantitatively measured at the same time, revealing that after 3 days, the heights of GA3-MN and GA3-Spray-treated tomato plants were 18%–21% higher than those of the WT or Control-MN plants (Figure S8). At the same time, the GA3-Injection plants showed an increase of around 10% in height (Figure S8), which was less effective than the GA3-MN or GA3-Spray groups. After 6 days, GA3-treated (including the GA3-MN, GA3-Spray, and GA3-Injection) plants showed an increase of 20%–43% in height compared to the non-treated controls (Figure 2E). The GA3-Injection group is again slightly less effective than GA3-MN or GA3-Spray. A similar trend was also observed on Day 9 (Figure S8B) and Day 15 (Figure S9). In particular, on Day 15, the GA3-MN group eventually outgrew all other control groups (Figure S9). In our test, direct injection of GA3 into the tomato stem by a syringe did not promote plant growth to the same extent as leaf spray or MN delivery. This is probably due to the fact that the direct stem injection method is very hard to control, where a precision control of injection rate is required to avoid liquid overflow. In contrast, the MN approach is much easier to apply without the need for flow rate control and therefore is more suitable for field or greenhouse applications.

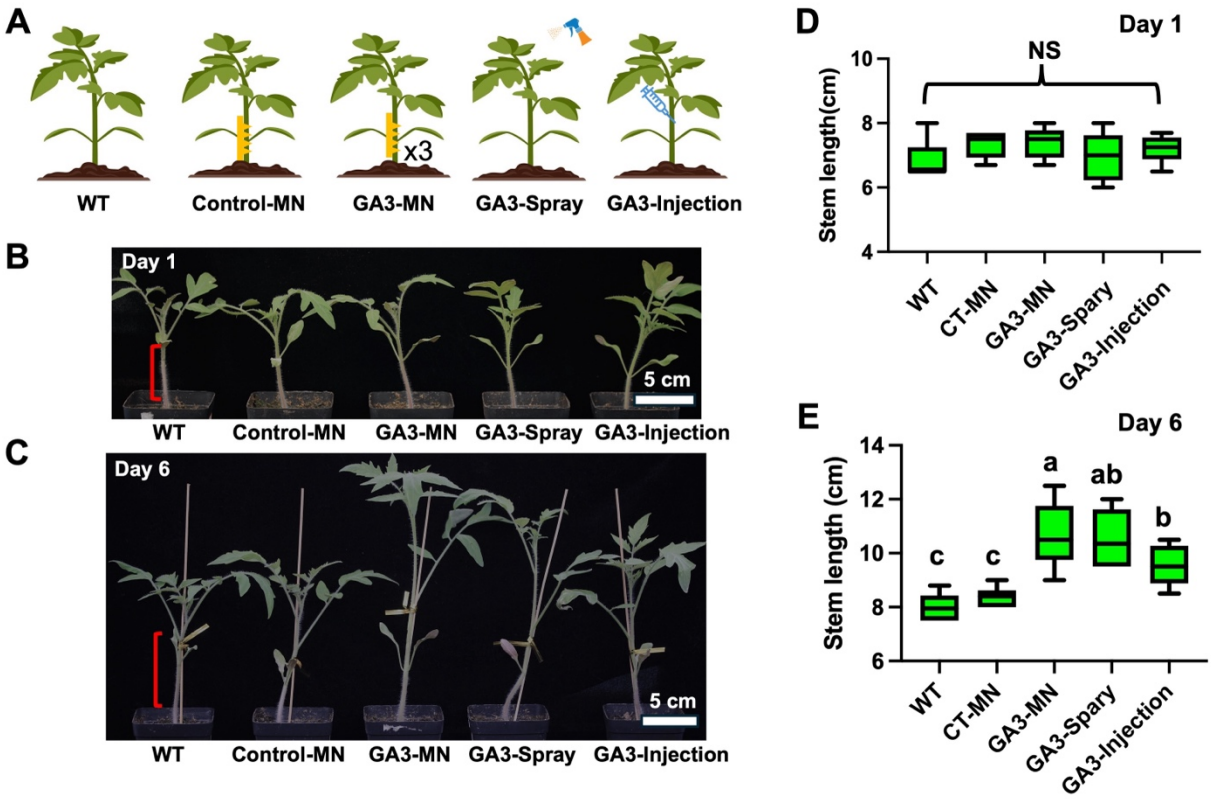

Figure 2. Tomato growth phenotype under different GA3 treatments. A) Schematic of different GA3 treatment methods on 25-day-old tomato plants. B,C) The growth phenotype of tomato plants at Day 1 and Day 6, respectively. D) The stem length of the tomato plants at Day 1 under different GA3 stimulations (n=12). NS = not significant. E) The stem length of the tomato plants at Day 6 under different GA3 stimulations (n=12). Different letters above the bars indicate statistically significant differences between groups ($P < 0.05$). Groups that share a letter are not significantly different ($P > 0.05$). CT = control.

We also tested the effect of the application frequency of GA3-MN treatment on tomato growth (Figure S10). The tomato plants for the MN injection experiment were divided into three groups, which received one (1x), two (2x), and three times (3x) of injections, respectively. All plants were injected on the first day; then, the second and third groups were injected again after three days; only the third group received a final injection after six days. Plant height was measured simultaneously throughout the experiment. The results showed that for GA3 delivery, one MN treatment is sufficient to promote tomato growth (Figure S10). On Day 6 and Day 9, the plant

292 height in group 2 and group 3 with more injections revealed larger variations compared to group
293 1 with only 1x MN injection (Figure S10B). These results demonstrated that for GA3 delivery by
294 PVA- MN, the application frequency can be as low as 1x.

295 Furthermore, GA3 delivery by PVA MN could also be performed on the lateral branch by
296 using 40-day-old tomato plants (Figure S11A and B). The injection process is the same as the stem
297 treatment. Due to the difference in the initial length of each lateral branch, we calculated the
298 relative lateral branch elongation to evaluate the GA3 stimulation. The results showed that after 3
299 days of treatment, the average lateral branch of GA3-MN and GA3-Spray-treated tomato plants
300 grew around 5% more than the WT and Control-MN plants (Figure S11C); after 6 days post-
301 injection, the average lateral branch length of the GA3-MN group increased by nearly 10% of the
302 control groups (Figure S11D).

303 In addition to the stem or branch growth length difference, we observed that the tomato
304 plants in GA3-treated groups (GA3-MN or GA3-Spray) showed a noticeable color difference from
305 the 4th to 6th compound leaf (newly emerging leaves) (Figure S12A). We assume that this
306 phenotype difference is probably due to the accelerated growth triggered by GA3. The
307 concentrations of chlorophyll a ($p = 0.0049$) and b ($p = 0.0025$) in the 4th to 6th leaves (mixed
308 samples) were also quantified. The results showed that in GA3-treated tomato, the leaf chlorophyll
309 a and b content decreased by 6% to 10% compared with WT and Control-MN plants (Figure S12B
310 and C), suggesting a faster growth rate in GA3-treated groups.

311

312

313

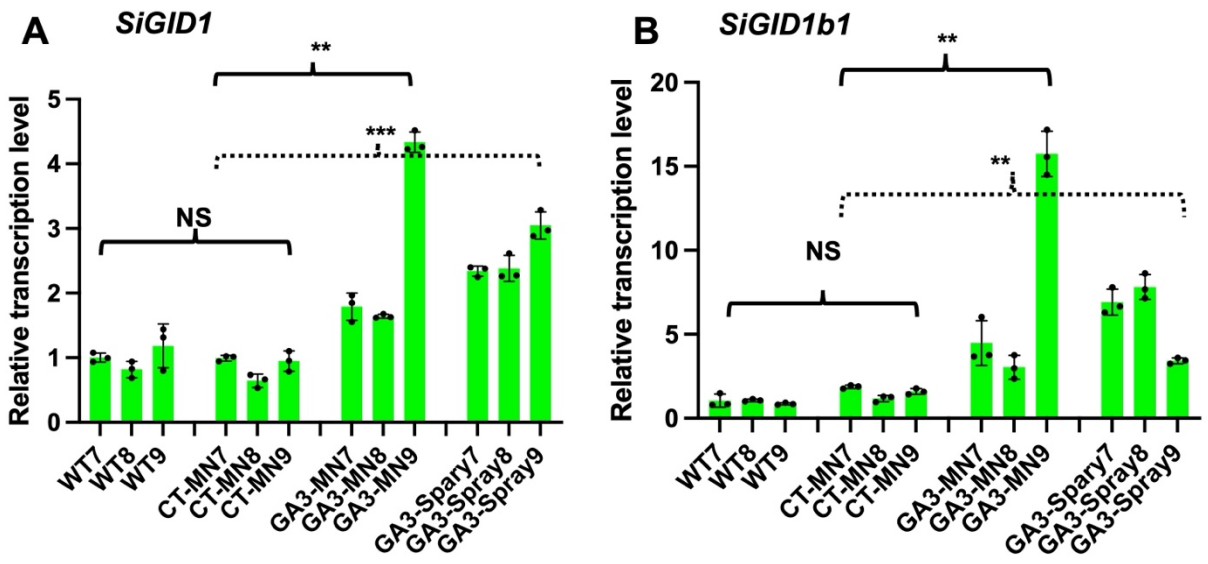

Figure 3. Tomato gene expression levels under different GA3 stimulations. A) The relative transcription level change of *SiGID1* genes under the different GA3 treatments in tomato plants. Each group has three different plant lines (plants 7, 8, 9). B) The relative transcription level change of *SiGID1b1* genes under the different GA3 treatments in tomato plants. Each group has three different plant lines (plants 7, 8, 9). CT = control. NS = not significant, *P < 0.05, **P < 0.01, ***P < 0.001.

To investigate whether the GA3-MN treatment would trigger the intrinsic gene transcription level changes in tomato plants. We conducted a series of reverse transcription-quantitative polymerase chain reaction (RT-qPCR) experiments using tomato leaf samples after different treatments. We selected the GA signal receptor, two tomato *GID* genes (Shohat et al., 2021), as targets and ran gene expression analysis. The results revealed that after GA3-MN or GA3-Spray treatments, both *SiGID1* and *SiGID1b1* genes showed significant increases in transcription level by 2 to 15-fold compared to the WT and Control-MN plants (Figure 3). The expression level of GA3-MN group is generally comparable to the GA3-Spray group (Figure 3). Interestingly, in individual plant #9, the MN treatment promoted higher *GID* gene expression level than conventional spraying. All the above data strongly suggest that the PVA-MN-GA3 injection promotes the stem or branch growth similarly to the foliar spray method, while reducing the

application dose by 10~20 times. Consistently, the gene expression involved in the GA3 signal in tomato plants was also upregulated, confirming the effectiveness of the delivery of GA3 by the MN patch into tomato plants.

PVA-MN for GA3 Delivery to *Arabidopsis ft-10 mutant*

Besides tomatoes, we also used a model plant *Arabidopsis thaliana* (*A. thaliana*) and investigated the PVA- MN injection effects on the GA3 signaling process. *A. thaliana* showed multiple advantages in phenotyping analysis such as well-characterized biological activities (including development, metabolism, hormone signaling, and stress responses), ease of genetic manipulation, and comprehensive genomic information.

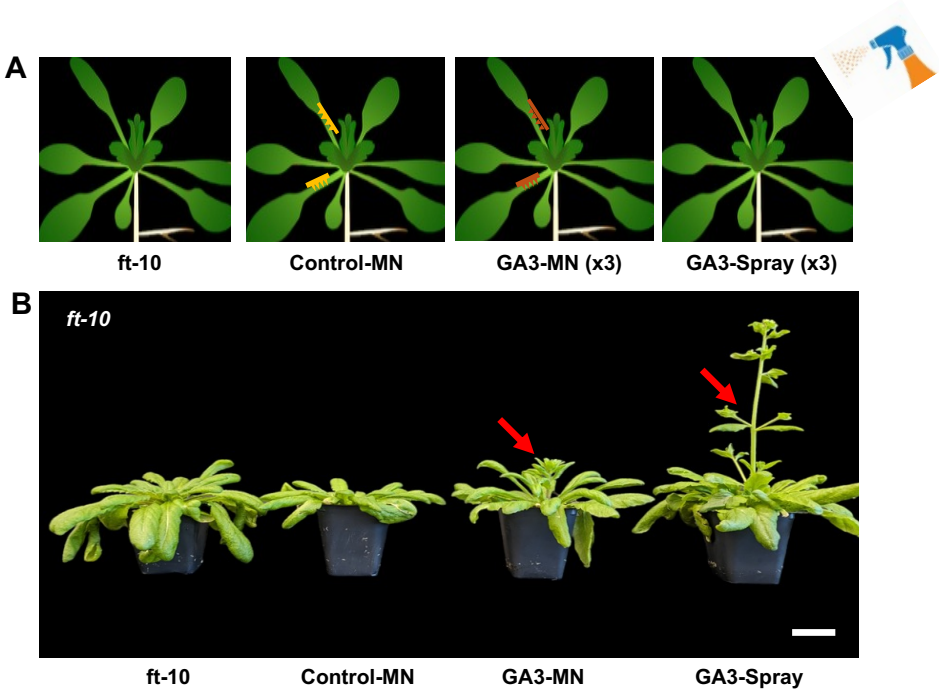

Figure 4: PVA-MN for GA3 delivery to *Arabidopsis ft-10* mutant. A) Schematic of different GA3 delivery methods to the *Arabidopsis ft-10* mutant. B) Representative image of *ft-10* plants 10 days after different GA3 treatments. MN injection and spray were carried out every three days. 4 groups of *ft-10* (n=5 for each group) were treated differently (including *ft-10*, Control-MN, GA3-MN, and GA3-Spray).

350 Numerous studies have shown that applying gibberellins (such as GA3) in *A. thaliana*
351 promotes the termination of vegetative growth, regulates flower formation, accelerates bolting,
352 and results in plants with fewer rosette leaves and more cauline leaves (Bao et al., 2020). Under
353 normal conditions, wild-type *A. thaliana* Col-0 plants produce around 14 rosette leaves during the
354 vegetative growth phase before inflorescence emergence at approximately 23 days under a 16-
355 hour light regime. Some studies report 11–13 rosette leaves between days 21–24 (Cao *et al.*, 2023).
356 Cao and colleagues studied the *Arabidopsis ft-10* mutant, a *FT* gene loss-of-function mutant with
357 a clear late-flowering phenotype under long-day conditions, to evaluate their silk-based
358 microneedle delivery system (Cao *et al.*, 2023). This mutant disrupts non-GA3-related pathways
359 that predominantly regulate flowering under long-day conditions (Figure S13A). Unlike the
360 previous silk-based microneedles, our study applied PVA-MN to the petiole of a single rosette leaf
361 in *Arabidopsis* plants (Figure S13B, C). The PVA- MN used in this experiment was 800 μm in
362 length.

363 To assess the effectiveness of PVA-MN in delivering GA3 to *Arabidopsis* plants, we again
364 compared MN-mediated delivery with foliar spray. Additionally, an empty PVA-MN (without
365 GA3) was used as a negative control (Control-MN, Figure 4A). GA3 was delivered via PVA-MN
366 injections at multiple leaves every 3 days, for a total of three applications (x3), similar to the
367 frequency of foliar sprays. For MN injection on *Arabidopsis* vein, a small array of 2 x 10 needles
368 was used. The leaf spray method used 2~4 mL of GA3 solution instead. The total GA3 amount
369 delivered by the spray method is nearly 10 times that used in the MN injection methods (Table1).
370 We observed that both GA3-Spray and GA3-MN treatments resulted in an early bolting phenotype
371 compared to the *ft-10* mutant control and the Control-MN group (MN without GA3) (Figure 4B).
372 Although GA3-MN-treated plants bolted earlier than the controls, their response was slower than
373 that of GA3-Spray-treated plants. It is because *Arabidopsis* exhibits a distinct, two-stage
374 developmental pattern, in which vegetative growth precedes reproductive growth. Initially, the
375 plant dedicates its energy to forming a rosette. The main stem's internodes remain compressed
376 during this entire phase. Once it receives the necessary environmental and internal cues, the plant
377 undergoes a critical phase transition that initiates rapid, dramatic elongation of the central stem,
378 known as bolting. In our experiment, the PVA-MN injection was performed at the petiole site,
379 which is different from the previous injection into the stem of tomato plants. The diffusion of GA3
380 to the whole plant from the petiole site is likely slower than that injected directly into the stem.

Furthermore, for MN treatment, we injected only three out of more than twenty inflorescences, meaning the total GA3 applied in the GA3-MN group was significantly lower than that in the GA3-Spray group. All these may contribute to the different flowering time observed between the GA3-MN and GA3-Spray groups.

In addition, rosette and cauline leaf numbers were also recorded throughout the growth period. GA3-MN injections produced phenotypes in *ft-10* similar to those observed in GA3-Spray plants, with changes in rosette and cauline leaf numbers and leaf size (Figure 5A). These phenotypes were significantly different from those *ft-10* mutants untreated with GA3 (Figure 5A). This confirms that GA3 delivered via microneedles effectively altered plant metabolism. Interestingly, Control-MN plants (without GA3) produced fewer rosette leaves than the untreated *ft-10* mutant, suggesting that PVA- MN injection may induce some stress even in the absence of GA3 (Figure 5A). These phenotypic findings demonstrate that PVA-MN is effective in delivering GA3 to *Arabidopsis* plants and changes their growth behavior accordingly.

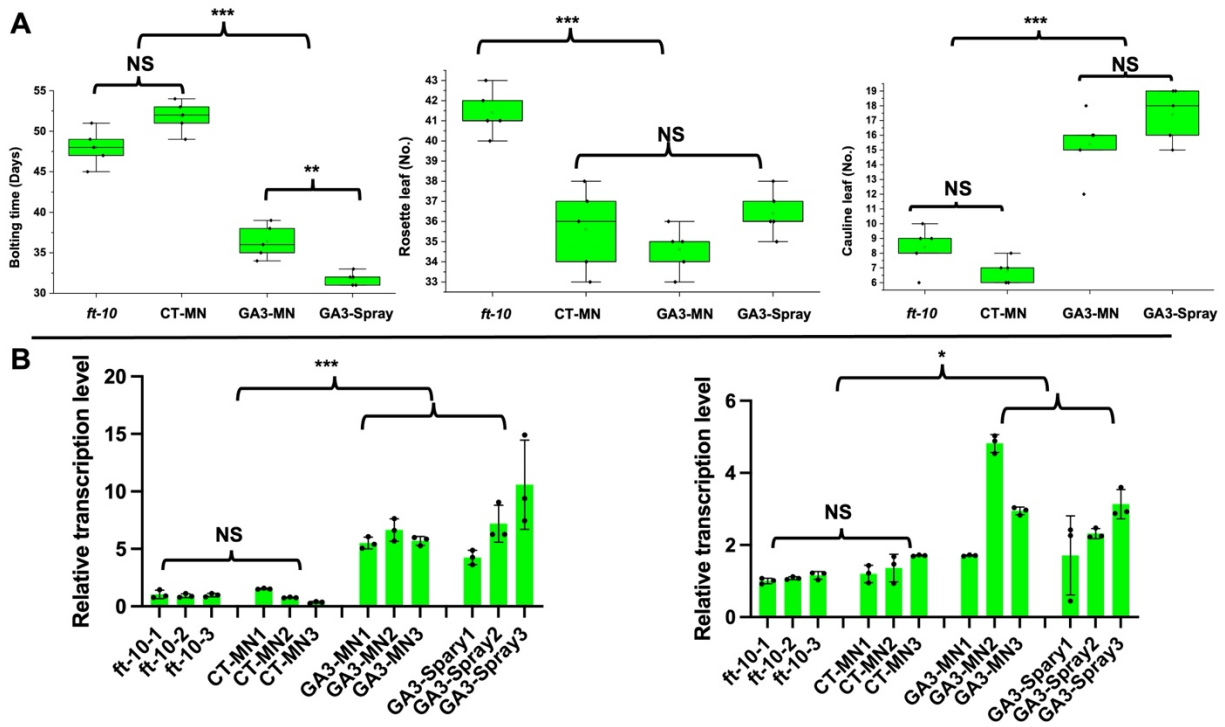

397 **Figure 5. Different GA3 delivery treatments alter *Arabidopsis* phenotype and gene expression**
398 **in the GA3 signaling pathway.** A) The bolting time, rosette leaf number, and cauline leaf number
399 change under different GA3 treatments in *Arabidopsis* ft-10 mutants. B) The relative transcription
400 level change of *AtGID1b* and *AtGID1c* genes under the different GA3 treatments in *Arabidopsis*
401 plant. Each group has three different plant lines (plants 1, 2, 3). CT = control; NS = not significant;
402 *P < 0.05, **P < 0.01, ***P < 0.001.

403

404 In *Arabidopsis* plants, there are three GA receptor isoform genes, namely *AtGID1a*, *1b,*
405 and *1c*. Using RT-qPCR, we analyzed transcript levels of these three genes with and without the
406 GA3-MN treatment (Figure 5B). We detected that the *AtGID1a* showed a low transcript level in
407 the *Arabidopsis ft-10* mutant background, but the other two GA receptor genes, the *AtGID1b* and
408 *AtGID1c*, showed a significant increase in the mRNA level by 2 to 10 fold after the GA3-MN and
409 GA3-Spray treatments (Figure 5B). These molecular results confirm the previous phenotypic
410 observations, suggesting that PVA-MN is an effective tool for delivering plant hormones in
411 *Arabidopsis*.

412

413 **Delivery of SA for induced TSWV resistance in *Nicotiana benthamiana* plant**

414 To test whether plant hormones can be successfully delivered into plants by using the MN,
415 we selected salicylic acid (SA) as a testing model and fabricated a PVA-MN patch loaded with 5
416 mM SA. SA is an important plant hormone that plays a significant role in triggering the pathogen
417 resistance response. To measure SA delivery efficiency, we used a 3 x 18 MN array applied to the
418 *Nicotiana Benthamiana* petiole with 2 min of contact time ("SA-MN"). At the same time, a 500
419 mM SA solution was sprayed on the leaf surface ("SA-Spray") or infiltrated into the leaf ("SA-
420 Infiltration") as the control (Figure 6A). Each *Nicotiana Benthamiana* plant was sprayed with 5-
421 10 mL of SA solution, and the injection volume for the SA-Infiltration method is approximately 1
422 mL. After 24 h of treatment, 100 mg of leaf tissue was sampled and ground in liquid nitrogen.
423 Plant tissue SA was isolated by an extraction buffer and analyzed by high-performance liquid
424 chromatography combined with a mass spectrometer (HPLC-MS).

The HPLC-MS/MS results showed that in WT and Control-MN plant leaves, there was very little SA (Figure 6B, Figure S14). In contrast, the leaves in the SA-MN, SA-Spray, and SA-Infiltration groups all showed relatively high SA concentrations (Figure 6B, Figure S14A). Notably, the SA-MN group showed a higher peak than the SA-Spray method (Figure 6B), indicating a higher delivery efficiency for the SA-MN method. We also quantified the SA concentrations in different samples. The results showed that leaves with SA-Infiltration had the highest SA content at 40 ng/g (Figure 6C). On the other hand, the MN-treated leaves accumulated a SA concentration of 14 ng/g, while the spray method only showed a SA concentration of 4 ng/g, the lowest among the three (Figure 6C). Overall, these results verify that the PVA-MN approach demonstrated a high delivery efficiency despite its low loading capacity.

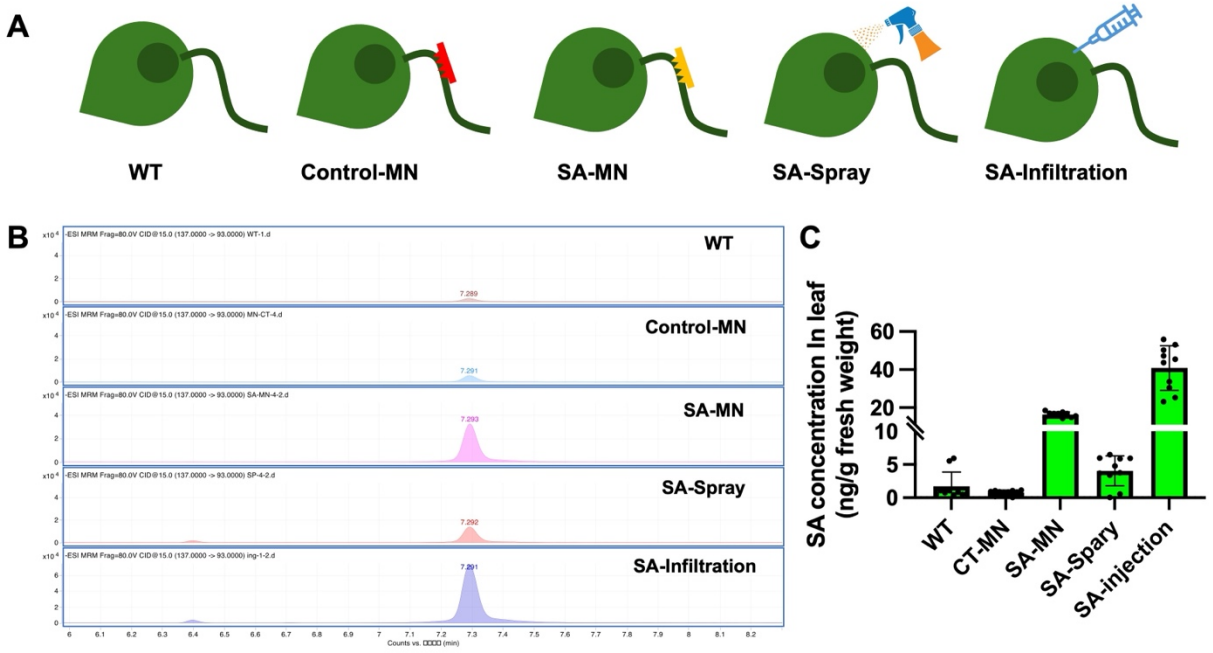

Figure 6. PVA-MN delivery of SA in *Nicotiana Benthamiana*. A) Schematic illustration of different SA delivery methods to *Nicotiana Benthamiana* plant on the petiole; Later, the dark region on the leaf was sampled for SA concentration analysis. B) HPLC-MS analysis showed the presence of SA (7.29 min) in leaf tissues with different delivery methods. C) The SA concentration

442 in different samples showed that PVA-MN has a higher delivery efficiency than the spray method.
443 (n=10). CT = control.

444

445 Tomato spotted wilt virus (TSWV) is a plant virus that belongs to the family *Tospoviridae*
446 and is one of the most economically significant plant viruses affecting crops worldwide (Best,
447 1968). The infected plants often show necrotic spots, wilting, chlorosis (yellowing), stunted
448 growth, leaf deformation phenotype, and in some cases, ring spots or concentric patterns on leaves
449 and fruits. These symptoms lead to reduced yield and poor fruit quality. Plant hormone SA has
450 been shown to play a significant role in triggering the resistance response to TSWV in plants
451 (Turina et al., 2016). SA is a crucial plant hormone involved in systemic acquired resistance (SAR),
452 a defense mechanism that provides broad-spectrum resistance to a variety of pathogens, including
453 viruses like TSWV (Durner et al., 1997). In the following experiment, we used PVA-MN to deliver
454 SA directly into plant tissues and investigated whether the MN microinjection could help the
455 model plant *Nicotiana Benthamiana* generate resistance to TSWV. Normally, the virus would
456 move within plants through a well-coordinated process that involves both cell-to-cell movement
457 and systemic movement via the plant's vascular system. To monitor TSWV movement in the plant,
458 TSWV infectious clone generated by Liu et al was engineered, and Cas9 in the infectious clone
459 was replaced with RUBY reporter (Liu et al., 2023), which makes the viral movement visible to
460 the naked eye (Figure S15).

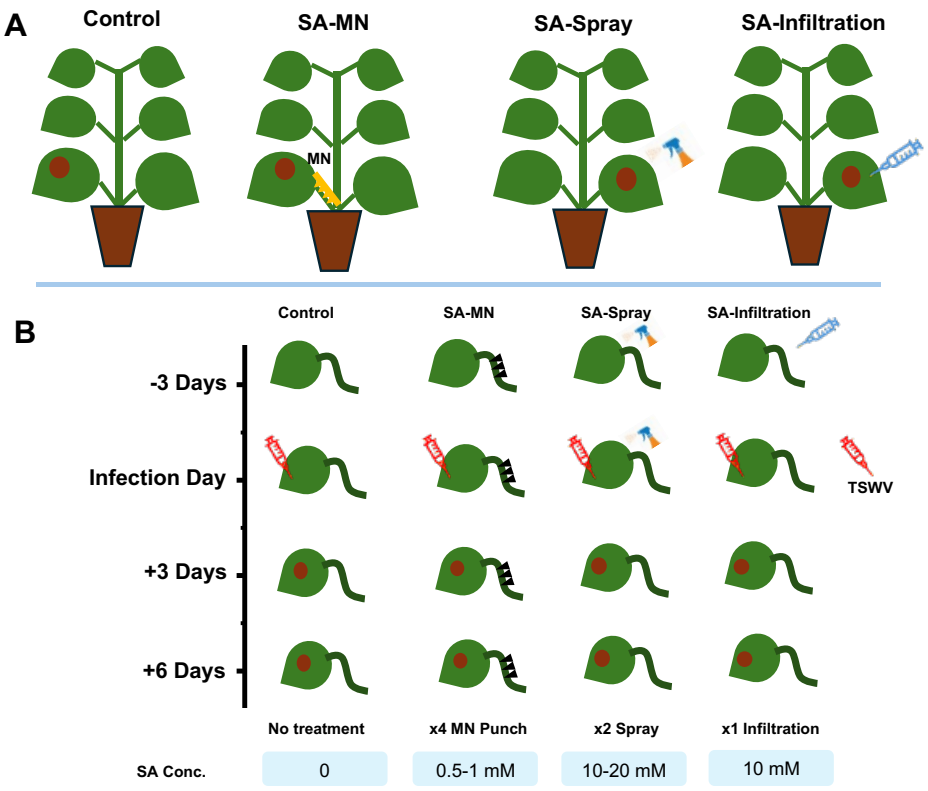

Figure 7. SA delivery to prevent TSWV virus movement in *Nicotiana benthamiana* plants. A) A schematic showing different SA delivery approaches. B) A treatment timeline showing the SA treatment process for SA-MN, SA-Spray, and SA-Infiltration methods in *Nicotiana benthamiana* plants, as well as the concentrations of SA used in different delivery approaches.

We compared the SA delivery and treatment efficiency of four different methods, including Control (no SA delivery), SA- MN, SA-Spray, and SA-Infiltration (Figure 7A). For SA- MN, the MN patch loaded with SA was applied to *Nicotiana Benthamiana* petiole for 4 times in total (1x before and 3x after TSWV inoculation). The SA-Spray method was performed 2 times (before and after inoculation), and the SA-Infiltration method was only performed once on *N. Benthamiana* (Figure 7B). For PVA-MN injection, a small MN array of 4x10 needles was used. The spray and infiltration treatments used 20-25 mL and 8-10 mL of SA solutions, respectively. The absolute amounts of SA delivered to tobacco plants by different delivery methods are summarized in Table 1.

476 In the first trial, the SA-MN group contained 2 mM SA, while the SA-Spray and SA-
477 Infiltration groups used only 500 μM SA, considering their larger application volumes. Still, the
478 estimated amount of SA delivered to the plants by the MN approach is only about 0.5-1% of the
479 spray or infiltration method (Table 1). Four *Nicotiana Benthamiana* plants were used for each
480 treatment, and three leaves were randomly selected from each plant for viral inoculation. During
481 the infection process, the gradual deepening of RUBY pigmentation was observed, indicating the
482 progression of viral infection. On the third- and sixth-days post-inoculation, we recorded the
483 numbers of lightly and deeply colored leaves to estimate the strength of the immune response in
484 the tobacco leaves. Three days after inoculation of *N. Benthamiana* plants with TSWV, we
485 observed virus infection in all test groups. However, the percentage of light-red (indication of
486 strong resistance) and dark-red (indication of weak resistance) leaves is quite different among the
487 groups. In the Control group, 8 among the total 12 (~67%) of the infected leaves turned dark-red
488 color. However, only 2 or 3 among total 12 (~21%) of the leaves showed dark color in SA-treated
489 plants (Figure 8A). There are no major differences between SA-MN, SA-Spray, and SA-
490 Infiltration groups. After 6 days, nearly 92% of the infected leaves were dark red in the Control
491 group. In contrast, the percentage of dark-red leaves in SA-treated groups was kept lower at around
492 50% (Figure 8A).

493 This indicates MN is a highly effective delivery platform for sending SA into leaf tissues
494 and inducing TSWV resistance. It is also interesting to note that after 15 days of viral infection,
495 all infected leaves turned a dark red color and died due to virus infection. The petioles of Control,
496 SA-Spray and SA-Infiltration groups all turned red color (Figure 8B), indicating the transport of
497 TSWV along the plant vasculature system. However, the SA-MN treated petiole remained green
498 (Figure 8B), indicating a strong viral resistance and fewer viral transport in the SA-MN treated
499 petiole tissue.

500

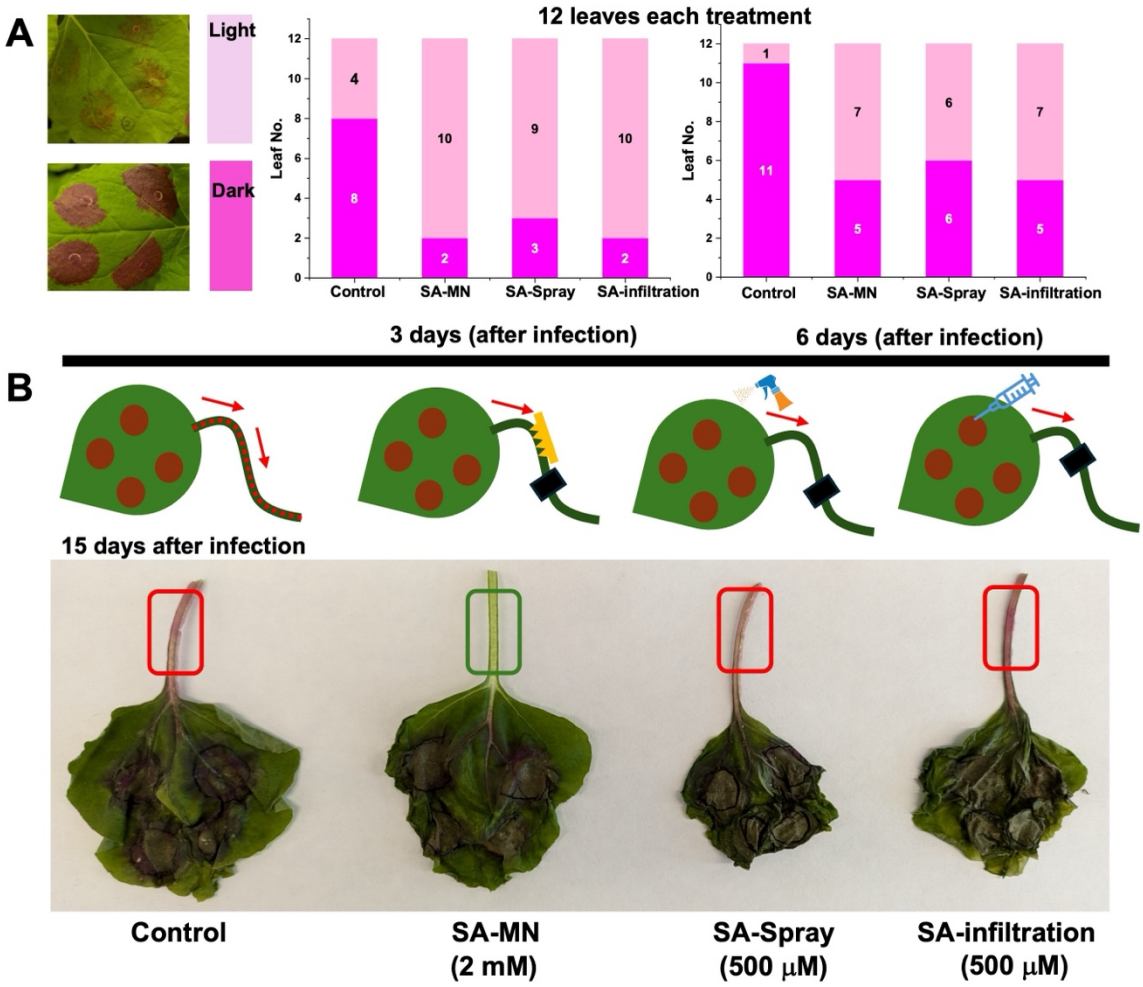

Figure 8. SA-MN delivery prevents TSWV movement in *Nicotiana Benthamiana*. A) TSWV infection in *N. benthamiana* leaf after 3 days and 6 days of inoculation, respectively, as evident by the expression of RUBY. The light-red color indicated less TSWV infection, while the dark-red color indicated higher TSWV load and less pathogen resistance. B) The phenotype of TSWV infected-*Nicotiana benthamiana* leaves (15 days post infection). SA-MN delivery inhibited the TSWV movement from the leaf to the petiole.

The comparison experiments were repeated by increasing the concentration of SA in SA-Spray and SA-Infiltration groups to 1 mM instead of 500 μM (Figure S16A). After 20 days of infection, the Control group clearly showed that the movement of TSWV from the leaf tissue to the stem, along the vein in the WT *Nicotiana Benthamiana* plants (Figure S16B). However, in SA-

513 MN, SA-Spray, and SA-Infiltrated plants, no red color on the stem was observed (Figure S16B).
514 After 30 days of infection, the Control plant revealed a dwarf phenotype compared to the SA-
515 treated plants (Figure S17A). The stem of Control plants showed tissue wilting. On the contrary,
516 the SA-MN and SA-Spray treated plants were still healthy, while some viral infection (red color)
517 was also found in SA-Infiltrated plants (Figure S17B), which may be due to less total SA treatment
518 dose in the infiltration method (Infiltration: 5 mL of 1 mM SA; Spray: 10 mL of 1 mM SA and
519 repeated 2x).

520 These experiments strongly suggested that SA could be effectively delivered to *Nicotiana*
521 *Benthamiana* plants by the MN delivery method and induce resistance to TSWV infection.
522 Compared to the traditional spray method, although the SA-MN method is more frequently applied
523 (totally 4x) and has a higher SA concentration (2 mM), it significantly reduces the total application
524 dose by ~99% (Table 1) while achieving similar immunization effects. Moreover, the spray
525 method required multiple treatment sites, including applications to the adaxial and abaxial sides of
526 the leaf, while the PVA-MN injection simply works on the stem or petiole. This suggests that our
527 PVA- MN delivery method not uses less active ingredient but also could be potentially applied
528 faster due to easier application locations.

529

530 **Discussion**

531 In this study, we demonstrated that PVA microneedle (MN) patches could be effectively utilized
532 as a precision plant delivery system for various compounds, including small-molecule dyes,
533 growth factors, and antiviral hormones (Figure 9). Compared to conventional delivery methods
534 such as foliar spray and soil application, which suffer from high chemical losses, environmental
535 impact, and low absorption (Boonupara *et al.*, 2023; Sinha *et al.*, 2022; Zeng *et al.*, 2021), PVA-
536 MN offer a promising alternative that can directly deliver target molecules into plant tissues with
537 high precision and low application dose and environmental side effects.

538 Our results show that PVA MN successfully delivered fluorescent dyes into tomato stem
539 vascular tissues, demonstrating their ability to penetrate plant tissues and promote compound
540 diffusion (Figure 1). This highlights the advantage of PVA-MN in enhancing plant uptake and

transport of bioactive molecules, which are often limited by environmental factors and plant surface barriers. Wounding assessments indicated that although MN insertion causes initial mechanical damage, the negative effects on stems are temporary and can be recovered by the plant itself (Figure S1-S5). Delivery of GA3 via PVA-MN accelerated tomato stem growth and altered chlorophyll levels in new leaves, confirming effective hormone delivery (Figure 2). Compared with foliar spraying, MNs produced comparable or slightly improved growth responses while reducing GA3 usage by nearly 90%, indicating a more controlled and efficient delivery method. Upregulation of GA receptor genes further confirmed successful activation of hormonal signaling. In Arabidopsis ft-10 mutants, MN-mediated GA3 delivery induced early bolting similar to foliar spraying, validating MN efficiency in a model system (Figure 4). The increased expression of GA receptor genes underscores the potential of PVA-MN for precise regulation of plant growth and development in agricultural applications. Finally, the application of SA via PVA-MN in *N. benthamiana* demonstrated the MN's ability to enhance plant resistance against TSWV, a new way of plant immunization with high accuracy (Figure 8). The restricted viral movement in SA-treated plants highlights the effectiveness of MN in delivering antiviral compounds directly to the infection site, thereby enhancing the plant's natural defense mechanisms. This approach offers a targeted method to combat viral infections, potentially reducing the need for broad-spectrum chemical treatments that can harm the environment.

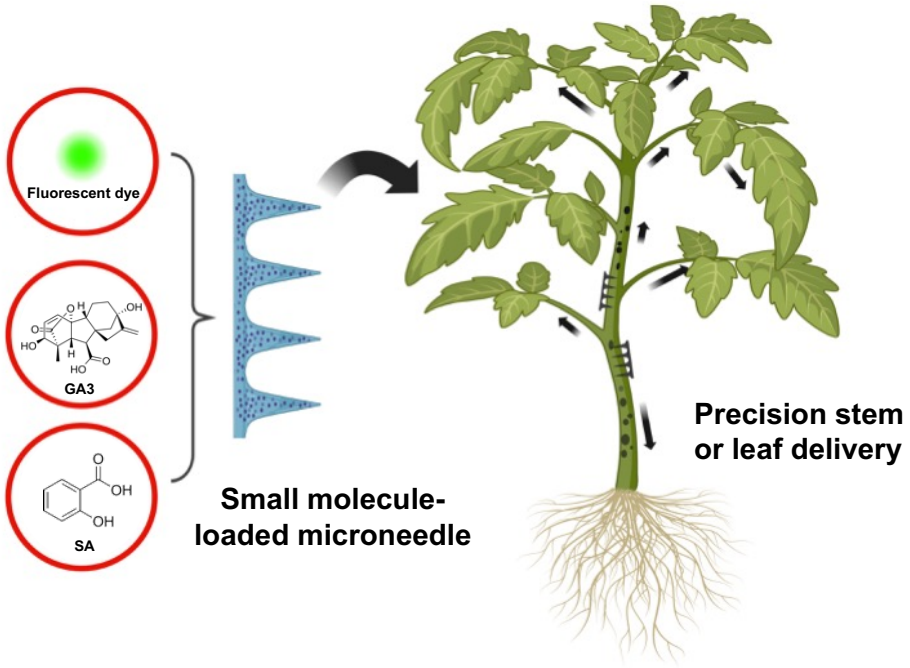

560 **Figure 9. Summary of different cargos delivered by the PVA-MN platform into a live plant**
561 **in this study.**

562

563 Our PVA-MNs differ from several previously reported microneedle systems used in
564 agriculture. For example, Cao and colleagues designed a silk-based microneedle platform (Cao *et*
565 *al.*, 2023; Cao *et al.*, 2020) that can also deliver small molecules and Agrobacterium to leaf tissues.
566 However, a major limitation of their approach is that the fabrication process for silk microneedles
567 is more complex and the production cost is much higher than that of our PVA-MNs.

568 On the other side, while several emerging nanomaterial-based delivery methods have been
569 demonstrated for delivering small molecules as well as DNA fragments and even proteins
570 (Demirer et al., 2021) to plants, these approaches are more suitable for small-scale laboratory
571 studies. Their overall cost is higher than that of PVA MNs, and their scalability is comparatively
572 more limited (Beig *et al.*, 2022; Demirer et al., 2019; Demirer et al., 2020). In addition, while
573 nanomaterials may enhance delivery at the cellular level, at the tissue level, many nanomaterials
574 still rely on foliar spray or infiltration-based delivery approaches. As the initial demonstration of
575 using PVA MNs for molecular delivery in plants, we only selected several small molecules such
576 as plant hormones for validation in this study. In the near future, MN also holds great promise for
577 the delivery of large biomolecules—including DNA, RNA, and proteins, even the gene editing
578 systems—into plant tissues.

579 Compared with existing or other emerging plant delivery methods, the MN approach
580 demonstrates obvious advantages. Owing to their simple fabrication, low cost, and environmental
581 safety, MN patches can be used for direct attachment to plant stems, petioles, or fruit pedicels for
582 localized delivery of nutrients, hormones, or protective agents. In greenhouse settings, MNs can
583 be deployed manually or via automated dispensers to achieve controlled and repeatable dosing. In
584 field applications, MN systems could be integrated with existing agricultural machinery systems
585 for large-scale, site-specific treatment. Furthermore, the smart polymer matrix allows the design
586 of time-controlled or humidity-responsive release formulations, enabling sustained molecular
587 delivery under fluctuating environmental conditions. After use, PVA MNs can be dissolved in

588 water or degraded by various microorganisms under aerobic and anaerobic conditions, producing
589 CO_2 and H_2O rather than persistent plastic fragments, therefore minimizing microplastic
590 contamination in plant tissues or the surrounding environment (Malka and Margel, 2023; Nair and
591 Laurencin, 2007; Tokiwa and Calabia, 2007). Together, these features demonstrate the feasibility
592 of applying MN technology in precision agriculture to enhance crop health and productivity while
593 minimizing environmental impacts.

594 Despite these promising results, several challenges remain in implementing MN-based
595 delivery methods in future. For instance, the dehydration effect observed in MN-treated leaf tissues
596 suggests that MN application may be more suitable for stems or stronger plant tissues. Stem
597 delivery may potentially also accept a larger amount of payloads and transport the delivered
598 payloads faster to other parts of the plant than leaf delivery. Moreover, due to the hydrophilic
599 properties of PVA, it is essential to maintain the stability and activity of loaded biomolecules
600 within the PVA matrix, which requires further optimization of the microneedle formulation.

601 In the future, the integration of PVAMN technology with agricultural robotics offers
602 another direction for next-generation precision crop management. As field robots and autonomous
603 platforms continue to advance in sensing, navigation, and manipulation (Oliveira et al., 2021;
604 Vougioukas, 2019; Wakchaure et al., 2023), MN-based delivery systems could be incorporated
605 into robotic arms or end-effectors to enable fully automated, site-specific treatment of individual
606 plants. Such systems could autonomously diagnose nutrient deficiencies, pathogen infections, or
607 growth abnormalities using onboard imaging and sensor networks, followed by immediate,
608 localized intervention through MN-mediated delivery with minimal human involvement. The soft
609 and adaptable nature of PVA-MN patches also makes them compatible with gentle robotic grippers,
610 reducing the risk of mechanical damage during automated application. In large-scale production
611 systems, fleets of robotic units could deploy MN patches with high precision and consistency,
612 allowing repeated or need-based delivery that responds dynamically to plant developmental stages
613 or environmental fluctuations. This convergence of MN-based biochemical delivery and
614 intelligent robotic actuation holds the potential to create a highly responsive, data-driven
615 agricultural framework that maximizes resource efficiency while minimizing chemical and labor
616 input.

In summary, our findings suggest that PVA-MNs are a viable and effective tool for plant compound delivery, offering benefits over traditional methods in terms of precision, efficiency, and reduced environmental impact. Future research should focus on scaling up MN fabrication processes, automating delivery techniques, and expanding the range of compounds that can be effectively delivered through this innovative system. With continued development, MN delivery technology could revolutionize precision agriculture, enabling more sustainable and targeted interventions in crop management.

Materials and methods:

Plant materials and growing conditions

Arabidopsis thaliana *ft-10* mutant seeds (TAIR Germplasm CS9869) and ecotype Columbia (Col-0) seeds were sterilized by soaking for 1 min in 70% ethanol and then for 10 min in 20% bleach, followed by five to seven rinses with sterile distilled water. Sterilized seeds were placed on Murashige and Skoog (MS) plates and kept at 4 °C for 2 days. The plate was placed in a plant growth chamber (Caron 7304-22-1) at 22 °C with long day (day/night 16h/8h) conditions, 70–100% relative humidity, and light intensity of 100 μmol m^{-2} s^{-1}. Seedlings were transferred to pots (2.5 × 2.5 × 3 in^3) with soil (Miracle-Gro Moisture Control Potting Soil Mix) on day 7 and watered regularly. Tomato (*Solanum lycopersicum* var. Beefsteak) seeds were purchased from The Seed Plant. Tomato seeds were grown in pots (3.5 × 3.5 × 3 in^3) in the plant room under long day (day/night 16h/8h) at 80 μmol m^{-2} s^{-1}, 70–90% relative humidity, day and night temperatures of 26 and 20 °C, respectively. *Nicotiana benthamiana* plants were grown in the growth chamber under 12h day and 12h night cycles at 26°C and 275 μmol m^{-2} s^{-1}.

TSWV virus infection

Agrobacterium tumefaciens GV3101 carrying recombinant plasmids (pL, pM-RUBY, pS-NSs, and triple VSR (viral suppressor of RNAi) were grown in Luria Broth media containing appropriate antibiotics (Rifampicin (50 μg/ml), Kanamycin (50 μg/ml), and Gentamycin (50 μg/ml)) for overnight. Cells were harvested from overnight grown cultures of *Agrobacterium* and re-suspended into the infiltration buffer (10 mM $MgCl_2$, 10 mM MES pH 5.6 and 100 μM

645 acetosyringone) at OD600 of 1 and further incubated at 28ºC for 3 hours. Before infiltration,
646 *Agrobacterium* cultures carrying pL, pM-RUBY, pS-NSs, and triple VSR plasmids were mixed at
647 final OD600 of 0.25. Three hours post-incubation, fully expanded *Nicotiana benthamiana* leaves
648 were co-infiltrated with *Agrobacterium* cells harboring pL, pM-RUBY, pS-NSs, and triple VSR
649 plasmids at final OD600 of 0.25 (Liu *et al.*, 2023).

650 **PVA MN fabrication process**

651 The microneedle patch was fabricated using a simple centrifugation method using
652 polydimethylsiloxanes (PDMS)-based negative molds (Blueacre Technology) in a 10 (w/v) %
653 polyvinyl alcohol (PVA) (M.W. 31,000-50,000, 98.0-98.8% hydrolyzed) (Acros Organics)
654 solution. To remove dust and debris from the micron-scale crevices of the PDMS molds, each chip
655 is first cleaned by repeated rinses with deionized (DI) water followed by two rounds of sonication
656 for 5 minutes each. The molds then dried at 35°C for 10-20 minutes to evaporate any remaining
657 water droplets clinging onto the needle edges. Next, 1.2 mL of PVA is allotted in 1.7 mL centrifuge
658 tubes, which undergo their first round of centrifugation at 6260g (Fisher Scientific accuSpin
659 Micro17) for 10 minutes remove any trapped air bubbles. The molds are then submerged in
660 degassed PVA solutions with the needle molds facing inwards and centrifuged again at 6260g for
661 10 minutes to fill the molds with PVA. The molds are then removed and sealed with another layer
662 of PVA to form a strong base for the needles upon drying. Lastly, the MN patches are partially
663 covered (for slow evaporation) and cured for 24 hours at room temperature to allow complete
664 solidification.

665 *MN patch fabrication with Gibberellic acid (GA3):* 34.6 mg of GA3 is dissolved in 500 µL
666 of dimethylsulfoxide (DMSO) and 500 µL of deionized (DI) water to make a stock solution of 100
667 mM of GA3. 6 µL of the solution is added to 1.2 mL of 10 (w/v) % PVA solution to make a final
668 GA3 concentration of 500 µM in 10 (w/v) % PVA solution for one microneedle patch. Each 20 x
669 20 MN array is made from 500 µL PVA-GA3 solution. In the tomato treatment experiments, only
670 a 4 x 10 array was pressed to the plant stem due to the small size of plant stems. The estimated
671 amounts of total GA3 delivered to different plants by MN are summarized in Table 1.

672 *MN patch fabrication with Salicylic Acid (SA):* 11.04 mg of SA is dissolved in 15 mL of
673 DI water to make a stock solution of 5.33 mM. This solution is then added to 16 (w/v) % PVA
674 solution to make a final solution of 2 mM SA and 10% (w/v) PVA for microneedle fabrication.

675 *MN patch fabrication with Rhodamine and 5(6)-carboxyfluorescein diacetate (CFDA):* 52
676 mg of Rhodamine is dissolved in 1.2 mL DI water to make a stock solution of 0.09 M. On the
677 other hand, to make a stock solution of 0.27 M CFDA, 25 mg of the powder is dissolved in 200
678 µL of DMSO. 33 µL and 11 µL of the respective stock solutions were added to 30 mL of 10 (w/v) %
679 PVA to make a final solution containing 0.1 mM Rhodamine and CFDA, respectively, which was
680 used to fabricate the microneedles.

681 **Fluorescent dye delivery in tomato plants**

682 CFDA (1 mM) and rhodamine 6G (1 mM) were mixed with a DMSO solution at a volume ratio
683 of 1:100 when fabricating the PVA-MN. To monitor fluorescence signal from the delivery and
684 transport of CFDA and rhodamine 6G, cross-sections upstream and downstream along the petiole
685 were observed under a microscope with fixed light intensity and an exposure time of 20 ms. The
686 petiole was also sliced longitudinally to image the distribution profile of CFDA in the xylem.
687 Image analysis was performed using ImageJ 1.52i. Fluorescence intensity was used as a proxy for
688 the concentration of CFDA within the tested range, and fluorescence signals were integrated
689 radially.

690 **Plant hormone preparation**

691 GA3 Solution Preparation: A 0.1 M stock solution of GA3 was prepared by dissolving 34.6 mg
692 GA3 in 1 mL 75% ethanol solution. GA3 spray solution was prepared by diluting the stock solution
693 1000× to a final concentration of 100 µM. Silwet-77 was added to obtain a final concentration of
694 0.01% in the GA3 spray.

695 SA Solution Preparation: A 100 mM stock solution of SA was prepared by dissolving 138
696 mg SA in 1 mL 75% ethanol solution. The SA spray solution was prepared by diluting 100 mM
697 SA stock 1000× to the final concentration of 0.1×10^{-3} M. Tween-20 was added to obtain a final
698 concentration of 0.01% in the SA spray and used as a surfactant to promote SA absorption.

699

700 **RT-qPCR based gene expression analysis**

701 RT-qPCR analysis was performed using SYBR-Green PCR Master mix (Invitrogen, Carlsbad, CA,
702 United States) on a CFX96TM (Bio-Rad, California, CA, United States). Gene-specific primer
703 pairs and different thermal programs (Supplementary Table S1) were developed to compare
704 expression levels in *Arabidopsis*, tomato, and *N. benthamiana* plants. *Arabidopsis UBQ10* gene
705 and tomato *Actin* gene were used as reference controls for normalization. A pre-RT-qPCR analysis
706 showed that the reference gene expression is stable under the plant hormone treatments including
707 GA3. Amplified products were monitored using an optical reaction module (SYBR-green) and the
708 resulting amplified values of genes were normalized against those of references according to a
709 previous protocol for plants (Li et al., 2021). The steps of qPCR analysis were carried out following
710 the method described previously (Li *et al.*, 2021). The reaction system was composed of 12 μL
711 mixture, including: 10 μL of SYBR-green-preMix, 1.0 μL of 10 μM forward and reverse primer,
712 and 1.0 μL of cDNA template (Li et al., 2017). The thermal program followed the protocol of Bio-
713 rad SYBR-Green PCR Master-mix. The thermal program is 95 ºC for 30s, (95 ºC for 10s, 60 ºC
714 for 1 min) ×40, 65 ºC to 95 ºC with 0.5 ºC increments in 2s, 4 ºC. Three replicates were performed
715 for each gene expression analysis. All the primers were listed in Supplementary Table S1.

716

717 **Salicylic acid (SA) extraction from tobacco leaf and detection using the HPLC-MS/MS**

718 For SA analysis, approximately 100 mg of fresh leaf tissue is collected and ground into a fine
719 powder in liquid nitrogen. The powder is transferred into a 2-mL microcentrifuge tube and
720 extracted with 1.0 mL of extraction solvent (methanol:water:formic acid = 80:19:1, v/v/v),
721 followed by the addition of a known amount of internal standard. The mixture is vortexed for 1
722 min and sonicated in an ice-cooled ultrasonic bath for 10–15 min, then centrifuged at 15,000 g for
723 10 min. The supernatant is transferred to a new tube. The pellet is re-extracted with an additional
724 0.5 mL of extraction solvent, and the supernatants from both extractions are combined (total
725 volume ~1.5 mL). The extract was stored at -80°C before measurement or taken directly to SPE
726 purification if preferred.

727 The content of SA was measured on an HPLC–MS/MS System (SCIEX Triple Quad 5500)
728 equipped with a C18 column (Phenomenex, 4.6 × 250 mm, 5 μm). The injection volume was 5 μL

with a flow rate of 0.4 mL/min. The column pressure is 1800 Bar and a column temperature of 40°C. The flow channel is A:100% water and B：100% Acetonitrile. A total 12 min timetable is: Start at 95% A, 5% B; 1 min: 95% A, 5% B; 6 min: 5% A, 95% B; 7.5 min: 5% A, 95% B; 10 min: 95% A, 5% B; 12 min: 95% A, 5% B. The mass spectrometer was operated under negative ionic mode with the Electrospray Ionization (ESI). The gas temperature was set to 320°C. The gas flow rate was set to 6 L/min, and the temperature of sheath gas, with 11 L/min flow rate, was set to 350°C. The data were acquired and analyzed with Analyst software. The SA were identified by comparing the standard substances. In result analysis, the characteristic ion fragments of the SA were set as 137/93 or 137/65. We observed that the SA retention time is at 7.29 min, and the 137/93 peaks were the major primary and secondary ion fragments in our analysis method.

Funding: The authors sincerely thank the funding support provided by Kenan Institute and the Game-Changing Research Incentive Program for the Plant Sciences Initiative (GRIP4PSI).

Author Contribution:

M.L. contributed to experimental design, plant treatments, RNA extraction, analysis of all experimental data, figure preparation, and manuscript drafting. A.D.P. contributed to PVA-MN preparation. J.X. contributed the SEM characterization of PVA-MN. H.J. contributed to RNA extraction from the plant tissue and RT-qPCR analysis, and the manuscript editing. Z.Z. contributed to the tomato plant cultivation, GA3, SA treatment, and the SA extraction from the tomato plants. Y.H. and N.L. contributed the HPLC- MS/MS analysis of SA from plants. Y.L., L.G., and T.X. provided the HPLC- MS/MS platform and contributed to the SA concentration analysis in the plant. D. S. and A.E.W. helped construct the RUBY-TSWV and TSWV infection experiments. Q.W. perceived and designed the project, developed experimental plans, supervised data analysis and figure preparation. All authors contributed to the revision of the manuscript.

Acknowledgements:

The authors thank Dr. Wusheng Liu at NC State Department of Horticulture for helping with RNA extraction. We also thank Lydia Parks for developing the MN fabrication protocol.

Declaration of interests:

The authors declare that the research was conducted in the absence of any commercial or financial relationships that could be construed as a potential conflict of interest.

Reference:

Alkharabsheh, H.M., Seleiman, M.F., Battaglia, M.L., Shami, A., Jalal, R.S., Alhammad, B.A., Almutairi, K.F., and Al-Saif, A.M. (2021). Biochar and its broad impacts in soil quality and fertility, nutrient leaching and crop productivity: A review. Agronomy **11**:993.

Bao, S., Hua, C., Shen, L., and Yu, H. (2020). New insights into gibberellin signaling in regulating flowering in Arabidopsis. Journal of Integrative Plant Biology **62**:118-131.

Barłóg, P., Grzebisz, W., and Łukowiak, R. (2022). Fertilizers and fertilization strategies mitigating soil factors constraining efficiency of nitrogen in plant production. Plants **11**:1855.

Beig, B., Niazi, M.B.K., Sher, F., Jahan, Z., Malik, U.S., Khan, M.D., Américo-Pinheiro, J.H.P., and Vo, D.-V.N. (2022). Nanotechnology-based controlled release of sustainable fertilizers. A review. Environmental Chemistry Letters **20**:2709-2726.

Best, R.J. (1968). Tomato spotted wilt virus. Advances in virus research **13**:65-146.

Boonupara, T., Udomkun, P., Khan, E., and Kajitvichyanukul, P. (2023). Airborne pesticides from agricultural practices: A critical review of pathways, influencing factors, and human health implications. Toxics **11**:858.

Brichi, L., Fernandes, J.V., Silva, B.M., Vizú, J.d.F., Junior, J.N., and Cherubin, M.R. (2023). Organic residues and their impact on soil health, crop production and sustainable agriculture: A review including bibliographic analysis. Soil Use and Management **39**:686-706.

Cao, Y., Lim, E., Xu, M., Weng, J.K., and Marelli, B. (2020). Precision delivery of multiscale payloads to tissue-specific targets in plants. Advanced Science **7**:1903551.

Cao, Y., Koh, S.S., Han, Y., Tan, J.J., Kim, D., Chua, N.H., Urano, D., and Marelli, B. (2023). Drug delivery in plants using silk microneedles. Advanced Materials **35**:2205794.

Cunningham, F.J., Goh, N.S., Demirer, G.S., Matos, J.L., and Landry, M.P. (2018). Nanoparticle-mediated delivery towards advancing plant genetic engineering. Trends in biotechnology **36**:882-897.

Davis, K.F., Gephart, J.A., Emery, K.A., Leach, A.M., Galloway, J.N., and D'Odorico, P. (2016). Meeting future food demand with current agricultural resources. Global Environmental Change **39**:125-132.

Demirer, G.S., Zhang, H., Goh, N.S., González-Grandío, E., and Landry, M.P. (2019). Carbon nanotube–mediated DNA delivery without transgene integration in intact plants. Nature protocols **14**:2954-2971.

Demirer, G.S., Zhang, H., Goh, N.S., Pinals, R.L., Chang, R., and Landry, M.P. (2020). Carbon nanocarriers deliver siRNA to intact plant cells for efficient gene knockdown. Science advances **6**:eaaz0495.

Demirer, G.S., Silva, T.N., Jackson, C.T., Thomas, J.B., W Ehrhardt, D., Rhee, S.Y., Mortimer, J.C., and Landry, M.P. (2021). Nanotechnology to advance CRISPR–Cas genetic engineering of plants. Nature Nanotechnology **16**:243-250.

Dimkpa, C.O., Fugice, J., Singh, U., and Lewis, T.D. (2020). Development of fertilizers for enhanced nitrogen use efficiency–Trends and perspectives. Science of the Total Environment **731**:139113.

Durner, J., Shah, J., and Klessig, D.F. (1997). Salicylic acid and disease resistance in plants. Trends in plant Science **2**:266-274.

Ece, E., Eş, I., and Inci, F. (2023). Microneedle technology as a new standpoint in agriculture: Treatment and sensing. Materials Today.

Faraji Rad, Z. (2023). Microneedle technologies for food and crop health: recent advances and future perspectives. Advanced Engineering Materials **25**:2201194.

Fukase, E., and Martin, W. (2020). Economic growth, convergence, and world food demand and supply. World Development **132**:104954.

Gupta, R., and Chakrabarty, S. (2013). Gibberellic acid in plant: still a mystery unresolved. Plant signaling & behavior **8**:e25504.

Han, Y., Jangir, M., Ngoh, A.S.Y., Li, C., Sarangapani, S., Cao, Y., Zhang, Y., Cheerlavancha, R., Sarojam, R., and Marelli, B. (2025). Precise Delivery of Physiological Doses of Melatonin in Planta to Control Postharvest Physiology and Extend Shelf Life Outside the Cold Chain. Nano Letters.

He, J., Wang, Y., Li, H., Ma, J., Yue, X., Liang, X., Hong, Y., Wang, F., Hu, C., and Liu, R. (2025). Controlled-Release Fertilizer Improving Paddy Yield and Nitrogen Use Efficiency by Reducing Soil Residual Nitrogen and Leaching Losses in the Yellow River Irrigation Area. Plants **14**:408.

Hina, N.S. (2024). Global meta-analysis of nitrate leaching vulnerability in synthetic and organic fertilizers over the past four decades. Water **16**:457.

Jakhar, A.M., Aziz, I., Kaleri, A.R., Hasnain, M., Haider, G., Ma, J., and Abideen, Z. (2022). Nano-fertilizers: A sustainable technology for improving crop nutrition and food security. NanoImpact **27**:100411.

Jung, J.H., and Jin, S.G. (2021). Microneedle for transdermal drug delivery: current trends and fabrication. Journal of pharmaceutical investigation:1-15.

Krishnasree, R., Raj, S.K., and Chacko, S.R. (2021). Foliar nutrition in vegetables: A review. Journal of Pharmacognosy and Phytochemistry **10**:2393-2398.

Li, M., Li, Y., Guo, L., Gong, N., Pang, Y., Jiang, W., Liu, Y., Jiang, X., Zhao, L., and Wang, Y. (2017). Functional characterization of tea (Camellia sinensis) MYB4a transcription factor using an integrative approach. Frontiers in Plant Science **8**:943.

Li, M., He, X., La Hovary, C., Zhu, Y., Dong, Y., Liu, S., Xing, H., Liu, Y., Jie, Y., Ma, D., et al. (2021). A De Novo regulation design shows an effectiveness in altering plant secondary metabolism. Journal of Advanced Research.

Li, M., Dey, P.A., Cui, Q., Hsieh, T.-F., Summeetha, J., Xu, J., Wesley B. Bruce, Jonathan T. Vogel, Allen Sessions, Antonio Cabrera, et al. (2025). **Non-destructive seed genotyping via microneedle-basedDNA extraction**. Plant Biotecnology Journal doi: 10.1111/pbi.70055.

Liu, C., Zhou, H., and Zhou, J. (2021). The applications of nanotechnology in crop production. Molecules **26**:7070.

Liu, Q., Zhao, C., Sun, K., Deng, Y., and Li, Z. (2023). Engineered biocontainable RNA virus vectors for non-transgenic genome editing across crop species and genotypes. Molecular Plant **16**:616-631. 10.1016/j.molp.2023.02.003.

Malka, E., and Margel, S. (2023). Engineering of PVA/PVP hydrogels for agricultural applications. Gels **9**:895.

Nagarkar, R., Singh, M., Nguyen, H.X., and Jonnalagadda, S. (2020). A review of recent advances in microneedle technology for transdermal drug delivery. Journal of Drug Delivery Science and Technology **59**:101923.

Nair, L.S., and Laurencin, C.T. (2007). Biodegradable polymers as biomaterials. Progress in polymer science **32**:762-798.

Nair, R., Varghese, S.H., Nair, B.G., Maekawa, T., Yoshida, Y., and Kumar, D.S. (2010). Nanoparticulate material delivery to plants. Plant science **179**:154-163.

Niu, J., Liu, C., Huang, M., Liu, K., and Yan, D. (2021). Effects of foliar fertilization: a review of current status and future perspectives. Journal of Soil Science and Plant Nutrition **21**:104-118.

Nkebiwe, P.M., Weinmann, M., Bar-Tal, A., and Müller, T. (2016). Fertilizer placement to improve crop nutrient acquisition and yield: A review and meta-analysis. Field crops research **196**:389-401.

Oliveira, L.F., Moreira, A.P., and Silva, M.F. (2021). Advances in agriculture robotics: A state-of-the-art review and challenges ahead. Robotics **10**:52.

Paul, R., Ostermann, E., and Wei, Q. (2020). Advances in point-of-care nucleic acid extraction technologies for rapid diagnosis of human and plant diseases. Biosensors and Bioelectronics **169**:112592.

Paul, R., Ostermann, E., and Wei, Q. (2022). Rapid Extraction of Plant Nucleic Acids by Microneedle Patch for In-Field Detection of Plant Pathogens. In Plant Pathology: Method and Protocols, (Springer: pp. 77-90.

Paul, R., Ostermann, E., Chen, Y., Saville, A.C., Yang, Y., Gu, Z., Whitfield, A.E., Ristaino, J.B., and Wei, Q. (2021). Integrated microneedle-smartphone nucleic acid amplification platform for in-field diagnosis of plant diseases. Biosensors and Bioelectronics **187**:113312.

Salama, D.M., Abd El-Aziz, M., Rizk, F.A., and Abd Elwahed, M. (2021). Applications of nanotechnology on vegetable crops. Chemosphere **266**:129026.

Schemmer, A., Wolfram, J., Roodt, A.P., Bub, S., Petschick, L.L., Herrmann, L.Z., Stehle, S., and Schulz, R. (2024). Pesticide mixtures in surface waters of two protected areas in southwestern Germany. Bulletin of Environmental Contamination and Toxicology **112**:10.

Shohat, H., Eliaz, N.I., and Weiss, D. (2021). Gibberellin in tomato: Metabolism, signaling and role in drought responses. Molecular Horticulture **1**:15.

Sinha, E., Calvin, K.V., Kyle, P.G., Hejazi, M.I., Waldhoff, S.T., Huang, M., Vishwakarma, S., and Zhang, X. (2022). Implication of imposing fertilizer limitations on energy, agriculture, and land systems. Journal of environmental management **305**:114391.

Tokiwa, Y., and Calabia, B.P. (2007). Biodegradability and biodegradation of polyesters. Journal of Polymers and the Environment **15**:259-267.

Tudi, M., Daniel Ruan, H., Wang, L., Lyu, J., Sadler, R., Connell, D., Chu, C., and Phung, D.T. (2021). Agriculture development, pesticide application and its impact on the environment. International journal of environmental research and public health **18**:1112.

Turina, M., Kormelink, R., and Resende, R.O. (2016). Resistance to tospoviruses in vegetable crops: epidemiological and molecular aspects. Annual review of phytopathology **54**:347-371.

Vasundhara, D., and Chhabra, V. (2021). Foliar nutrition in cereals: A review. Pharma Innov J **10**:1247-1254.

Vougioukas, S.G. (2019). Agricultural robotics. Annual review of control, robotics, and autonomous systems **2**:365-392.

Wakchaure, M., Patle, B., and Mahindrakar, A. (2023). Application of AI techniques and robotics in agriculture: A review. Artificial Intelligence in the Life Sciences **3**:100057.

Wang, J.W., Cunningham, F.J., Goh, N.S., Boozarpour, N.N., Pham, M., and Landry, M.P. (2021). Nanoparticles for protein delivery in planta. Current opinion in plant biology **60**:102052.

Young, M.D., Ros, G.H., and de Vries, W. (2021). Impacts of agronomic measures on crop, soil, and environmental indicators: A review and synthesis of meta-analysis. Agriculture, Ecosystems & Environment **319**:107551.

Zeng, F., Zuo, Z., Mo, J., Chen, C., Yang, X., Wang, J., Wang, Y., Zhao, Z., Chen, T., and Li, Y. (2021). Runoff losses in nitrogen and phosphorus from paddy and maize cropping systems: A field study in Dongjiang Basin, South China. Frontiers in Plant Science **12**:675121.

Zhang, H., Zhang, H., Demirer, G.S., González-Grandío, E., Fan, C., and Landry, M.P. (2020). Engineering DNA nanostructures for siRNA delivery in plants. Nature protocols **15**:3064-3087.

Zhang, H., Cao, Y., Xu, D., Goh, N.S., Demirer, G.S., Cestellos-Blanco, S., Chen, Y., Landry, M.P., and Yang, P. (2021). Gold-nanocluster-mediated delivery of siRNA to intact plant cells for efficient gene knockdown. Nano letters **21**:5859-5866.

Zhang, H., Goh, N.S., Wang, J.W., Pinals, R.L., González-Grandío, E., Demirer, G.S., Butrus, S., Fakra, S.C., Del Rio Flores, A., and Zhai, R. (2022). Nanoparticle cellular internalization is not required for RNA delivery to mature plant leaves. Nature nanotechnology **17**:197-205.

Zhang, L., Wang, J., Fan, Y., and Wang, Y. (2023). Coacervate-enhanced deposition of sprayed pesticide on hydrophobic/superhydrophobic abaxial leaf surfaces. Advanced Science **10**:2300270.

Zheng, L., Chen, H., Wang, Y., Mao, Q., Zheng, M., Su, Y., Xiao, K., Wang, K., and Li, D. (2020). Responses of soil microbial resource limitation to multiple fertilization strategies. Soil and Tillage Research **196**:104474.